



## Miscut measuring of SrTiO<sub>3</sub> single crystal using high resolution X-ray diffraction

Aziz M. Abdullah<sup>1</sup>, Salah R. Saeed<sup>1</sup>

<sup>1</sup> Department of Science, College of Basic Education I, University of Charmo, Chamchamal, Kurdistan Region, Iraq  
 E-mail: [aziz-muhemed@hotmail.de](mailto:aziz-muhemed@hotmail.de), [salah1966sh@gmail.com](mailto:salah1966sh@gmail.com)

### Article info

Original: 13 Jan. 2015  
 Revised: 18 Mar. 2015  
 Accepted: 19 Apr. 2015  
 Published online:  
 20 Sep. 2015

### Key Words:

Strontium titanate  
 (SrTiO<sub>3</sub>)  
 High resolution X-ray  
 diffraction  
 Substrate  
 Thin films  
 Miscut.

### Abstract

Strontium titanate (SrTiO<sub>3</sub>) is one of the perovskite type metal oxides with multi-functional properties and it has a lot of applications in various sectors of technology. In this paper, we obtained the miscut angles from Bragg peak after performing  $\omega$  scans of HRXRD at different angles of  $\phi$  with intervals of 90°. The obtained results located between 0.2015° and 0.4302° using two ways (mathematically and Epitaxy software), which is considered as a tolerance limit (less than 1°) to cut the substrates.

### Introduction

Strontium titanate (SrTiO<sub>3</sub>) is one of the perovskite class metal oxides with ABO<sub>3</sub> stoichiometry type crystal structure. Bulk Strontium titanate (STO) has space group Pm\_3m and cubic unit cell shown in **Figure: 1** with lattice constants of  $a = 3.901 \text{ \AA}$  [1] at room temperature (RT). This structure consists of two cations A and B and three oxygen anions, which can be characterized by alternating planes AO and BO<sub>2</sub> [2-5].

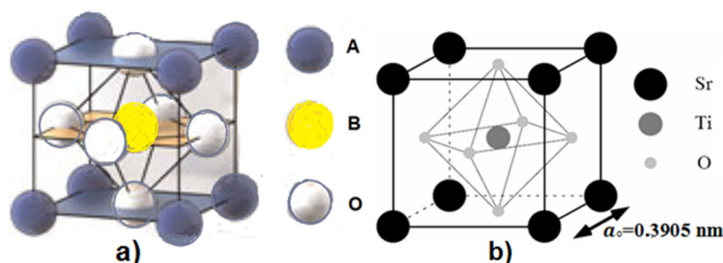


**Figure.1:** a) Cubic perovskite unit cell planes of AO and BO<sub>2</sub>, b) Atomic structure of (SrTiO<sub>3</sub>) at room temperature (RT). [4,5].

Due to multifunctional properties such as chemically inert, superconductivity, magnetism and ferroelectricity [6,7], STO is widely used in various sectors of technology as gas sensors, memory storage devices and layered high-Tc superconductors [8-10].

Highly crystalline substrate surface is necessary for the growth of thin films, which means, controlling the surface properties of substrate is very important in preparing high quality thin films [11-12]. But practically, it is impossible to cut the surface completely straight, which means that an angle is created between the surface and the planes. The produced angle is considered as a type of defect known as miscut.

The miscut of the substrate strongly affects certain properties (such as catalytic activities and dielectric and ferroelectric properties), which, in turn, influences the growth parameter of the thin film, and subsequently, in the design of various electroceramic devices, including capacitors and metal oxide semiconductors. This results attribute to the fact that the miscut stretches or compresses the film along the plane [13,14]. Due to the 1.9° miscut angle of the (001) SrTiO<sub>3</sub>, different domain and microstructures of the SrRuO<sub>3</sub> films are created as well as influences on the step flow growth of the thin film [15]. Chen and *et al.* [16] studied ferroelectric domain structure of BiFeO<sub>3</sub> on (001) SrTiO<sub>3</sub> substrate of 0.8° and 4° miscut angles, they found that the domain width increases with increasing miscut angles. All applications are sensitive to the purity of substrate crystal structure. The tolerance limit of the substrate miscut is regarded to be less than 1° [17,18]. In this work, the miscut studies of the substrate have been carried out using high resolution x-ray diffraction (HRXRD) of STO.

**Experimental**

The single crystal Strontium Titanate SrTiO<sub>3</sub> with a surface area of 10x10 mm<sup>2</sup> and a thickness of 1 mm, which is grown by the Verneuil technique [19], was purchased from crystal Technology GmbH–Berlin.

The as-grown single crystals were pretreated to obtain well defined single- terminated surface (001) [20,21]. In order to measure the miscut of the samples, a high- resolution X-ray diffractometer (Philips X pert system) were used with 1.6 kW incident X-ray beam and CuKα<sub>1</sub> line of wavelength λ = 0.15405 nm were selected using Ge220 four crystal monochromator [22-23]. The angle between the substrate surface and the index plane from the position of the substrate peak of (002) reflections in four rocking curves with (ω-scan) was recorded after (by) rotating the substrate in 90° steps in ϕ scan. The difference between the surface orientation and the orientation of the crystal is exactly defined as the miscut.

The miscut (γ) of STO (001) was calculated from two perpendicular components γ<sup>0,180</sup> and γ<sup>90,270</sup>. The first component represents a setting of the crystal lattice, satisfies Bragg’s law. The γ<sup>0,180</sup> was calculated from the relation:

$$\gamma^{0,180} = \frac{|\alpha^0 - \alpha^{180}|}{2} \dots\dots\dots (1)$$

where α<sup>0</sup> = ω - γ and α<sup>180</sup> = ω + γ are incidence angles of X-ray beam for azimuths of 0° and 180° (see Fig. 2). ω is the Bragg angle for interplanar spacing d<sub>002</sub>. The second component (γ<sup>90,270</sup>) was calculated using the relation:

$$\gamma^{90,270} = \frac{|\alpha^{90} - \alpha^{270}|}{2} \dots\dots\dots (2)$$

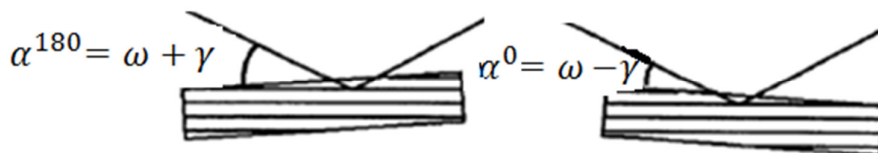


**Fig. 2:** Rotation of surface plane (002) by 180°.

The relation between angular deviation ( $\gamma$ ) and two azimuthal components  $\gamma^0$  and  $\gamma^{90}$  is described by the relationship [24]:

$$\cos\gamma = \cos\gamma^{0,180} + \cos\gamma^{90,270} \dots\dots\dots (3)$$

For very small angles, Eq (3) can be approximated by:

$$\gamma^2 = (\gamma^{0,180})^2 + (\gamma^{90,270})^2 \dots\dots\dots (4)$$

The diffraction angle  $\phi$  intensity, full width at half maximum (FWHM) and omega ( $\omega$ ) for STO samples are presented in Table1, The comparison of the calculated angular deviation ( $\gamma$ ) of all STO samples with the Epitaxy software Off-cut values is given in Table 2. An overview epitaxy software results for STO14 sample is shown in Table 3.

**Table 1:** The diffraction angle  $\phi$ , intensity, full width at half maximum (FWHM) and omega ( $\omega$ ) for all STO samples.

Sample	$\phi$ (°)	Intensity (a.u)	FWHM (°)	( $\omega$ ) (°)
STO 14	0	8090,3	0,0410	23,0322
STO 14	90	4839,8	0,0431	22,9892
STO 14	180	4361,2	0,0561	23,0904
STO 14	270	4234,0	0,0826	23,4162
STO 15	0	6354,3	0,0496	22,7903
STO 15	90	2967,6	0,0555	23,2392
STO 15	180	8912,5	0,0439	23,6502
STO 15	270	5908,3	0,0614	23,2493
STO 16	0	9307,1	0,0368	23,1348
STO 16	90	11358,6	0,0292	23,0516
STO 16	180	8242,9	0,0468	23,3202
STO 16	270	10674,6	0,0311	23,4064
STO 18	0	22280,9	0,0259	23,0492
STO 18	90	17550,4	0,0457	23,0968
STO 18	180	21946,8	0,0303	23,3809
STO 18	270	18586,1	0,0406	23,3214

**Table 2:** The comparison of the calculated angular deviation ( $\gamma$ ) of all STO samples with the Epitaxy software Offcut values.

Sample	$\alpha^0$	$\alpha^{180}$	$\gamma^{0,180}$	$\alpha^{90}$	$\alpha^{270}$	$\gamma^{90,270}$	$\gamma = \sqrt{(\gamma^{0,180})^2 + (\gamma^{90,270})^2}$	Epitaxy software Offcut (°)
	(°)	(°)	(°)	(°)	(°)	(°)	calculated mathematic	
STO14	23.3224	23.0904	0.116	22.9892	2.4162	0.2137	0.2429	0.2429
STO15	22.7898	23.6502	0.4302	23.2390	23.2491	0.0050	0.4302	0.4302
STO16	23.1351	23.3206	0.0927	23.0525	23.4106	0.1790	0.2015	0.2015
STO18	23.0487	23.3808	0.1660	23.0963	23.3487	0.1260	0.2084	0.2084

**Table 3:** An overview Epitaxy software results [Scan names,  $\omega$ ,  $2\theta$ ,  $\phi$  magnitude and Miller indices] for STO 14 sample. The similar procedure was taken for determining the off-cut of the other samples.

Scan Name	$(\omega)$ ( $^{\circ}$ )	$2\theta$ ( $^{\circ}$ )	$\phi$ ( $^{\circ}$ )	hkl
Scan 1: $\phi$ 0	23.32245	46.47150	0	002
Scan 3: $\phi$ 180	23.09100	46.46250	180	002
Scan 2: $\phi$ 90	22.98876	46.46500	90	002
Scan 4: $\phi$ 270	23.41602	46.46900	270	002

The diffraction curves for all studied samples STO14, STO15, STO16 and STO18 at different  $\phi$  (0, 90, 180, 270) $^{\circ}$  measurement using HRXRD and their miscuts value are presented in **Figs. 3-6**, respectively.

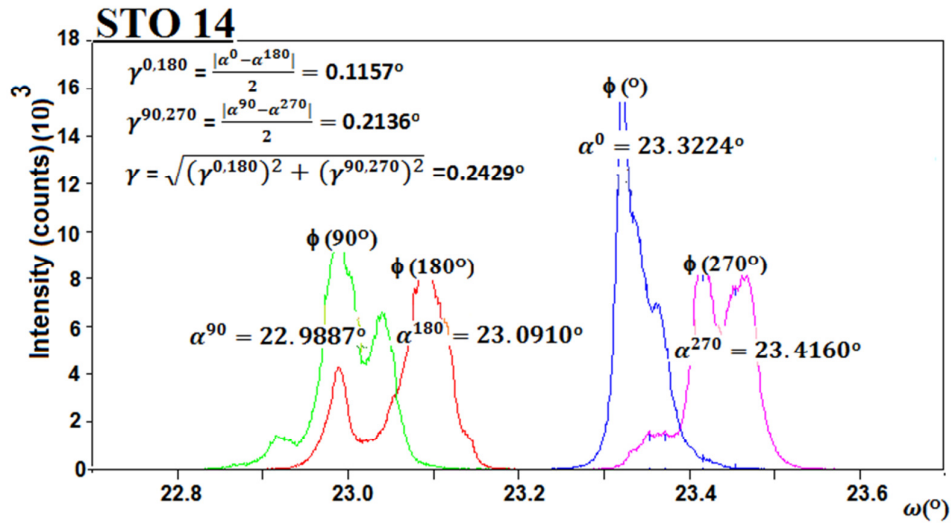


**Fig. 3:** The Combine graph of diffraction curves for different  $\phi$  (0, 90, 180, 270) $^{\circ}$  for STO14 measured by using the HRXRD. The miscut value: 0.2492 $^{\circ}$  is also presented.

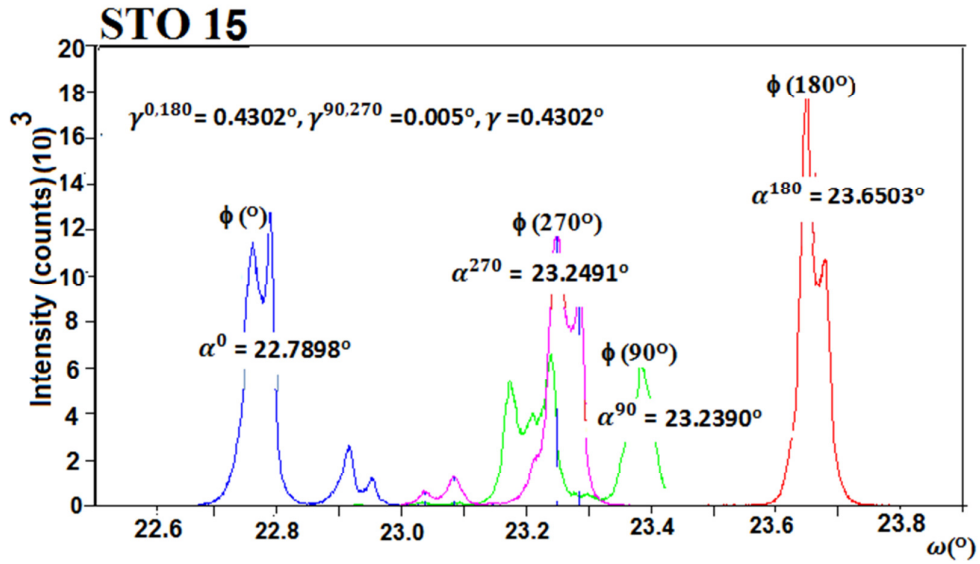


**Fig. 4:** The Combine graph of diffraction curves for different  $\phi$  (0, 90, 180, 270) $^\circ$  for STO15 measured by using the HRXRD. The miscut value:  $0.4302^\circ$  is also presented.

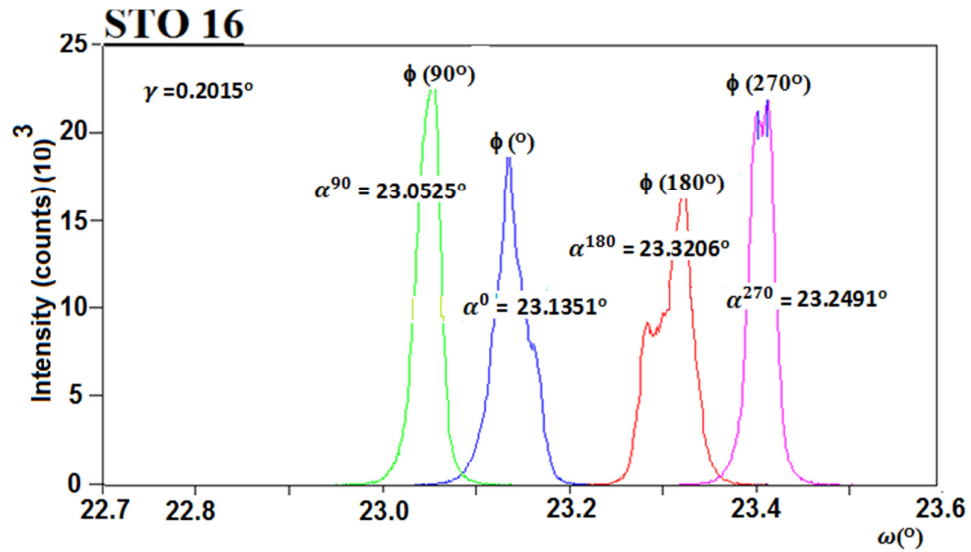


**Fig. 5:** The Combine graph of diffraction curves for different  $\phi$  (0, 90, 180, 270) $^\circ$  for STO16 measured by using the HRXRD. The miscut value:  $0.2015^\circ$  is also presented.

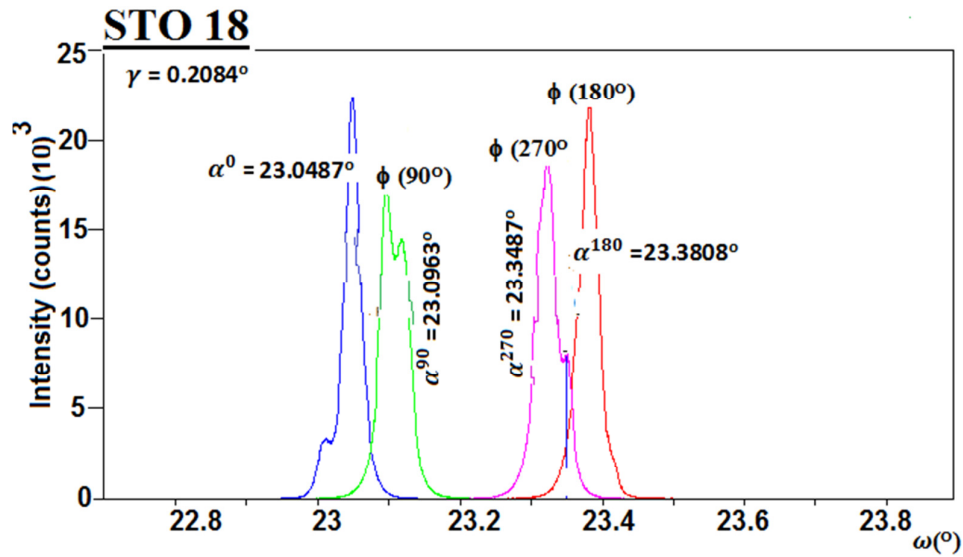


**Fig. 6:** The Combine graph of diffraction curves for different  $\phi$  (0,90,180,270) $^\circ$  for STO18 measured by using the HRXRD. The miscut value:  $0.2084^\circ$  is also presented

## Conclusion

The miscut of substrate surfaces of STO samples was measured by using the HRXRD technique. The obtained miscut angles are less than  $0.5^\circ$ , which reveals the tolerance limit to cut the substrates for depositing the film on it. The lower miscuts means the smaller surface steps which corresponds to atomic ally flat surfaces and the miscut already effects on the creation of microstructure on the deposited films. However, the polishing process improves the surface quality, but to overcome the surface miscut (ideal surfaces), we have to find the nano-techniques for sample cutting Nano cutter could be a promising candidate in future in one hand (microscopic limit) or other indestructive way.

## Acknowledgement

These measurements were carried out at Institute of Experimental Physics II- Faculty of Physics and Earth Sciences - Leipzig University. We acknowledge the staff and Prof. Michael Lorenz for fruitful discussion regarding this work and to the Department of Science - College of Education - Charmo University- Chamchamal.

## References

- [1] Muller, K. A., Berlinger, W. and Waldner, F., "Characteristic Structural Phase Transition in Perovskite-type Compounds", Phys. Rev. Lett., Vol. (21), pp. 814-817, (1968).
- [2] Bachelet, R., Sanchez, F., Santiso, J., Munuera, C., Ocal, C. and Fontcuberta, J., "Self-Assembly of SrTiO<sub>3</sub> (001) Chemical-Terminations: A Route for Oxide-Nanostructure Fabrication by Selective Growth", Chem. Mater, Vol. (21), pp. 2494-2498, (2009).
- [3] Peng, L., Xi, X., Moeckly, B. and Alpay, S., "Strain relaxation during in situ growth of SrTiO<sub>3</sub> thin films", Appl. phys. Lett. Vol. (83), pp. 4592-4594, (2003).
- [4] De Groot, F. M. F., Grioni, M., Fuggle, J.C., Ghijsen, J., Sawatzky, G. A. and Petersen, H., "Oxygen 1S x-ray-absorption edges of transition-metal oxides", Phys. Rev. B., Vol. (40), pp. 5715-5723, (1989).

- [5] Kuiper, B., Blok, J. L., Zandvliet, H. J., Blank, D. H. A., Rijnders, G. and Koster, G., "Self-organization of SrRuO<sub>3</sub> nanowires on ordered oxide surface terminations", MRS Communications, Vol. (1), pp 17-21. (2011).
- [6] Yoshimura, T., Fujimura, N. and Ito, T., "The initial stage of BaTiO<sub>3</sub> epitaxial films on etched and annealed SrTiO<sub>3</sub> substrates", J. Cryst. Growth, Vol. (174), pp. 790-795, (1997).
- [7] Moller, P. J., Komolov, S. A., Lazneva, E. F. "Selective growth of a MgO (100)-c (2x2) superstructure on a SrTiO<sub>3</sub>(100)-(2x2) substrate", Surf. Sci., Vol. (425), pp. 15-21, (1999).
- [8] Reagor, D. W. and Butko, V. Y., "Highly conductive nanolayers on strontium titanate produced by preferential ion-beam etching", Nat. Mat., Vol. (4), pp. 593-596, (2005).
- [9] Yamanaka, J., "Distribution of dislocations in SrTiO<sub>3</sub> single crystal", Mater. Trans., JIM, Vol. (40), pp. 915-918, (1999).
- [10] Yoshiikawa, M., "Dislocations in Hg<sub>1-x</sub>Cd<sub>x</sub>Te/Cd<sub>1-z</sub>Zn<sub>z</sub>Te epilayers grown by liquid-phase epitaxy", J. Appl. Phys. Vol. (63), pp. 1533-1540, (1988).
- [11] Adachi, H., Setsune, K. and Wasa, K., "Superconductivity in (La<sub>0.9</sub>Sr<sub>0.1</sub>)<sub>2</sub> CuO<sub>4</sub> single-crystal films", Phys. Rev. B., Vol. (35), pp. 8824-8825, (1987).
- [12] Hasegawa, H., Fukazawa, T. and Aida, T., "Contact between High-T<sub>c</sub> Superconductor and Semiconducting Niobium-Doped SrTiO<sub>3</sub>", Jpn. J. Appl. Phys., Vol. (28), pp. 2210 – 2212, (1989).
- [13] Blank, D. H. A., Rijnders, A. J. H. M., Schönherr, H., Broekmaat, J. J. and Bijl, D. B., "Nucleation and growth on SrTiO<sub>3</sub> substrates characterize by ex-situ AFM", (s0001465), (2007).
- [14] Cho, G., Yamamoto M., and Endo, Y., "Surface features of self-organized SrTiO<sub>3</sub> (001) substrates inclined in [100] and [110] directions", Thin Solid Films, Vol (464), pp. 80-84, (2004).
- [15] Jiang, J. C., Tian, W., Pan, X. Q., Gan Q. and Eon, C. B., "Domain structure of epitaxial SrRuO<sub>3</sub> thin films on miscut(001) SrTiO<sub>3</sub> substrate", Appl. phys. lett., Vol. (72), pp. 2963-2965, (1998).
- [16] Chen, Y. B., Katz, M. B. and *et al.* Pan, X. Q., Das, R. R., Kim, D. M., Baek S. H. and Eom, C. B., "Ferroelectric domain structures of epitaxial (001) BiFeO<sub>3</sub> thin films", Appl. Phys. Lett., Vol. (90), pp. 072907, (2007).
- [17] Zhang, Z. and Lagally, M. G., "Atomistic Processes in the Early Stages of Thin-Film Growth", Science, Vol. (276). pp. 377-383, (1997).
- [18] Chen, Y., "Microstructure of perovskite oxide thin films grown on miscut/small lattice-mismatched substrates", (Doctoral Dissertation), University of Michigan, (2008).
- [19] Koster, G., Rijnders, G., Blank, D. and Rogalla, H., "Surface morphology determined by (001) single-crystal SrTiO<sub>3</sub> termination, physica C: SrTiO<sub>3</sub> Superconductivity", Science, Vol. (339), pp. 215-230, (2000).
- [20] Kawasaki, M., Takahashi, K., Maeda, T., Tsuchiya, R., Shinohara, M., Ishiyama, O., Yonezawa, T., Yoshimoto, M. and Koinuma, H., "Atomic Control of the SrTiO<sub>3</sub> Crystal Surface", *Science*. Vol. (266), pp. 1540-1542, (1994).
- [21] Scheel, J. H., "Historical aspects of crystal growth technology", J. Cryst. Growth, Vol. (211), pp. 1-12, (2000).
- [22] Abdullah., A. M., "Structural Study of SrTiO<sub>3</sub> single crystal using High resolution X- ray diffraction", (JZS-A), Vol. (15). pp. 91-96,(2013).
- [23] Lorenz, M., Brandt, M., Wagner, G., Hochmuth, H., Zimmermann, G., von Wenckstern<sup>a</sup>, H. and Grundmann, M., "MgZnO: P Homoepitaxy by Pulsed Laser Deposition: Pseudomorphic Layer-by-Layer Growth and High Electron Mobility", Proc. SPIE 7217, Zinc Oxide Materials and Devices IV, 7217, 72170N, (2009).
- [24] **Sass, J., Mazur, K., Surma, B.,** Eichhorn, F., Litwin, D., Galas, J. and Sitarek, S., "X-ray studies of ultra-thin Si wafers for mirror application", Nucl. Instr. Meth. Phys. Res. B., Vol. (253), pp. 236-240, (2006).

